Biophysical Chemistry 151 (2010) 111–118

Contents lists available at ScienceDirect

Biophysical Chemistry

journal homepage: http://www.elsevier.com/locate/biophyschem

Optical studies of single-tryptophan *B. licheniformis* β-lactamase variants

Valeria A. Risso [a,b], María E. Primo [b,c], Juan E. Brunet [d], Carlos P. Sotomayor [d], Mario R. Ermácora [a,b,*]

[a] Departamento de Ciencia y Tecnología, Universidad Nacional de Quilmes, Roque Sáenz Peña 325, (1876) Bernal, Buenos Aires, Argentina
[b] Consejo Nacional de Investigaciones Científicas y Técnicas, Rivadavia 1917 (1033) Ciudad Autónoma de Buenos Aires, Argentina
[c] Cátedra de Inmunología, Facultad de Farmacia y Bioquímica, Universidad de Buenos Aires (UBA) and IDEHU (Conicet UBA), Junín 954 C1113AAD, Ciudad Autónoma de Buenos Aires, Argentina
[d] Pontificia Universidad Católica de Valparaiso, Instituto de Química, Avenida Parque Sur s/n, Curauma, Valparaiso, Chile

ARTICLE INFO

Article history:
Received 16 April 2010
Received in revised form 27 May 2010
Accepted 27 May 2010
Available online 2 June 2010

Keywords:
β-lactamase
Tryptophan fluorescence
UV-absorption
Circular dichroism
Protein conformation

ABSTRACT

β-lactamases (penicillinases) are important complicating factors in bacterial infections and excellent theoretical and experimental models in protein structure, dynamics and evolution. *Bacillus licheniformis* exo-small penicillinase (ESP) is a Class A β-lactamase with three tryptophan residues, one located in each of the two protein domains and one located in the interface between domains. To determine the tryptophan contribution to the ESP UV-absorption, circular dichroism, and steady-state and time-resolved fluorescence, four Trp→Phe mutants were prepared and characterized. The residue substitutions had little impact on the native conformation. UV-absorption and CD features were identified and ascribed to specific aromatic residues. Time-resolved fluorescence showed that most of the fluorescence decay of ESP tryptophans is due to a discrete exponential component with a lifetime of 5–6 ns. Fluorescence polarization measurements indicated that fluorescence of Trp 210 is nearly independent of the fluorescence of Trp 229 and Trp 251, whereas a substantial energy homotransfer between the latter pair takes place. The spectroscopic information was rationalized on the basis of structural considerations and should help in the interpretation and monitoring of the changes at the sub domain level during the conformational transitions and fluctuations of ESP and other Class A β-lactamases.

1. Introduction

β-lactamases cause a common bacterial resistance to antibiotics, a worrisome, world-wide health problem. Besides having medical, microbiological, and pharmaceutical interest, they are intensely studied as regards protein structure, dynamics, function, and evolution. Thus a deeper understanding of the properties of these proteins would benefit many areas of research.

ESP is a typical class A β-lactamase (Fig. 1). It possesses a single polypeptide chain of 265 residues organized in two domains. The α domain comprises the middle part of the sequence and is made of α helices; the α + β domain includes the sequence termini and contains a five-stranded β-sheet and two α-helices [1]. The catalytic mechanism of ESP has been thoroughly investigated [2–4], and high-resolution structures and biochemical evidence have shown that it involves a transient acylation of a serine residue at the active site, which is characteristic of all class A β-lactamases. Moreover, ESP is thermodynamically very stable and under denaturing conditions populates several partially folded states [5–11].

The fluorescence of tryptophan residues is widely used as a probe in kinetic and equilibrium studies of protein folding. By studying steady-state and time-resolved fluorescence emission, anisotropy, lifetime, and quenching, it is possible to assess molecular motion, association, solvent accessibility and structural fluctuation [12–15]. Likewise, the UV absorption of tryptophan residues is a very useful tool for monitoring protein conformation and dynamics [16–18]. ESP has three tryptophan residues, and its optical properties represent a complex combination of signals emanating from diverse parts of the molecule (see Fig. 1). Whereas the average spectroscopic signals still allow the assessment of the overall properties of the different conformational states, this complexity becomes a limitation for interpreting specific conformational changes of the different substructures of the molecule.

To overcome that limitation, we sought to simplify the optical properties of ESP. Three variants of ESP were prepared in which two of the three tryptophan residues were replaced by phenylalanine. We named these variants ESP^{W210}, ESP^{W229}, and ESP^{W251}, to indicate explicitly the position in the sequence at which the lone tryptophan residue is located. Also, a fourth variant that lacks tryptophan residues altogether was prepared: $ESP^{\Delta W}$.

The above variants were characterized and compared with the wild type protein, and a report on their catalytic, structural, and spectroscopic behavior is given. It was established that several of the spectral

Abbreviations: BP, benzylpenicillin; CD, circular dichroism; ESP, *B. licheniformis* exo-small penicillinase; PAGE, polyacrylamide gel electrophoresis; NATrpA, *N*-acetyl-L-tryptophanamide; NATyrA, *N*-acetyl-L-tyrosinamide.

* Corresponding Author. Departamento de Ciencia y Tecnología, Universidad Nacional de Quilmes, Roque Sáenz Peña 325, (1876), Bernal, Buenos Aires, Argentina. Tel.: +54 114 365 7100; fax: +54 114 365 7131.
E-mail address: ermacora@mail.unq.edu.ar (M.R. Ermácora).

0301-4622/$ – see front matter © 2010 Elsevier B.V. All rights reserved.
doi:10.1016/j.bpc.2010.05.013

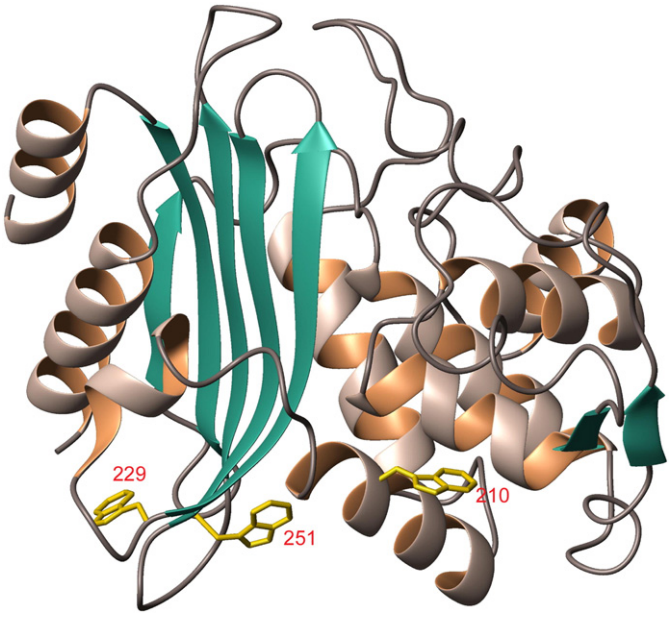

Fig. 1. Cartoon structure of ESP. The α + β and α domains are at the left and right sides, respectively. The three tryptophan residues of wild type EPS are labeled.

properties of ESP can be deduced from the spectral contributions of the single tryptophan residues in the variants and that these contributions report on the structure with subdomain resolution. We are now in the position of relating specific conformational details of this model protein to particular optical signals. The new knowledge in turn will greatly facilitate the design of experiments for addressing a number of unsolved issues in the folding behavior of this protein, such as the conformational nature of its equilibrium folding intermediates, the features of its folding pathway, and the cooperative behavior of its two domains.

2. Materials and methods

2.1. General details

Benzylpenicillin (BP) was purchased from Sigma (St. Louis, Missouri). Protein purity was assessed by SDS-PAGE. Circular dichroism (CD) and analytical size-exclusion chromatography were carried out as described [7]. Enzymic activity was determined spectrophotometrically ($\Delta\,\varepsilon_{240\ nm} = 570\ M^{-1}\ cm^{-1}$) at 25 °C in 50 mM sodium phosphate, pH 7.0 supplemented with 1.5 μM bovine serum albumin and the desired concentration of BP [19]. Microsoft Excel 2000 was used to fit equations to the data. Mass analysis was performed on a VG Quatro II (VG Biotech, Altrinchan, UK) triple quadrupole instrument equipped with an electrospray ionization source. Accessible surface area (ASA) of the tryptophan residues was calculated with a 1.4 Å probe according to the method of Richards [20]. The measurement theoretically estimates the solvent accessibility of these residues assuming that they conserve in the mutants the conformation and packing observed in the wild-type X-ray structure (4blm.pdb).

2.2. Protein expression and purification

In previous works [6,8,11], ESP (UniProtKB accession number P00808, E.C. = 3.5.2.6) was referred to as 'ESBL' (exo small β-lactamase). Herein, the name has been changed to ESP to avoid the confusion with 'extended spectrum β-lactamase', also abbreviated ESBL and widely used in the literature.

The cDNAs for ESP^{W210}, ESP^{W229}, ESP^{W251}, and $ESP^{\Delta W}$ were prepared by PCR mutagenesis using *Pfx* DNA polymerase (Invitrogen CA, USA), appropriate primers, and pELB3 as a template [5]. PCR products were cut with restriction enzymes and ligated into XbaI/BamHI sites of pET9a generating $pELB3^{W210}$, $pELB3^{W229}$, $pELB3^{W251}$, and $pELB3^{\Delta W}$. *Escherichia coli* BL21 (DE3) cells transformed with pELB3 and its derivatives were grown in Luria Bertani medium at 37 °C to $A_{600\ nm} \sim 1.0$. Finally, ESP variants were overexpressed by a 3-h induction with 1 mM isopropyl β-D-1-thiogalactopyranoside or 1% lactose and harvested by centrifugation.

ESP and the tryptophan variants were purified by a published protocol [7]. Briefly, cells (10 g) were osmotically shocked by incubation in cold water, the isolated osmotic shock fluid (~900 ml) was mixed with one tenth volume of 100 mM sodium acetate, pH 5.0 at 4 °C, and loaded into a fast-flow SP Sepharose column equilibrated with 10 mM sodium acetate, pH 5.0 (Buffer A). Elution was performed with a 150-ml linear gradient between 0–250 mM NaCl in Buffer A. The fractions containing β-lactamase activity were dialyzed against water at 4 °C and finally lyophilized.

2.3. Hydrodynamic and unfolding studies

Size exclusion chromatography was carried out at 22 °C with a FPLC Superose 12 10/30 column, equilibrated with 100 mM sodium phosphate, pH 7.0 (Buffer B), and UV detection at 280 nm (Pharmacia, Uppsala, Sweden). Stokes radii (R_S) were calculated from a calibration curve with standard proteins [21].

Unfolding transitions as a function of temperature were monitored by CD at 220 nm. Protein concentration was 1.5 μM, and a 1.0-cm cell was used. The temperature was varied linearly from 0 to 95 °C at a 2 °C-min^{-1} rate, and the melting curve was sampled at 0.2-min intervals. The following equations were fit to the data [22]

$$\begin{aligned}\Delta G_{NU} &= -RT\,In\left(\frac{f_U}{f_N}\right) \\ &= \Delta H_{Tm} + \Delta_{Cp}(T - T_m) \\ &\quad -T\left[\left(\frac{\Delta H_{Tm}}{T_m}\right) + \Delta C_p In\left(\frac{T}{T_m}\right)\right]\end{aligned} \tag{1}$$

and

$$S = f_N(S_{0,N} + l_N T) + f_U(S_{0,U} + l_U T), \tag{2}$$

where f_U and f_N are the unfolded and folded fractions at equilibrium and $f_U + f_N = 1$, T_m is the temperature at which $f_U = f_N$, S is the observed CD signal, $S_{0,N}$ and $S_{0,U}$ are the intrinsic CD signals for the native and unfolded state respectively, l_N and l_U are the slopes for the assumed linear dependence of $S_{0,N}$ and $S_{0,U}$ with the temperature. CD buffer was 25 mM sodium phosphate, 100 mM sodium fluoride. The fit was performed simultaneously for pH 6.0, 7.0 and 8.0, with a global ΔC_P and pH-specific energy and baseline parameters.

2.4. Optical studies

The molar extinction coefficients of ESP and its variants were determined as described previously [17]. UV-absorption spectra (240–340 nm, 0.1 nm sampling interval, 20 nm/s) were obtained with a Jasco V-550 spectrophotometer (Jasco Corporation, Japan). Ten spectra for each sample were averaged, blank corrected, and scaled to the corresponding molar extinction coefficient. The data were then smoothed using a 10-point moving-window and a fourth-degree polynomial filter [23]. Finally, the fourth-derivative of the spectra was calculated applying two successive cycles of second order derivation [17].

Circular dichroism spectra were obtained at 20 °C on a Jasco J-810 spectropolarimeter (Jasco Corporation, Japan) equipped with a Peltier effect device for temperature control. Scan parameters were 20 nm/min, 1-s response time, 0.2-nm data pitch, and 1-nm bandwidth. CD buffer was 25 mM sodium phosphate, 100 mM sodium fluoride, pH 7.0. Near-UV measurements were carried out with a 1.0-cm light-path length and protein concentration was 15-μM. In the far-UV, a 0.1-cm light-path

length was used and the protein concentration was 1.5 μM. Ten scans were averaged for each sample and the corresponding blanks subtracted. The final spectra were smoothed using a forty-point moving window and a fourth order polynomial [23].

Steady-state and time-resolved fluorescence were measured with K2 spectrofluorometers (ISS, Champaign, IL). Protein solutions were prepared in Buffer B. A quantum counter in the reference channel was used to correct lamp fluctuations. Excitation was at 295 nm (8 nm bandwidth). The quantum yields (Φ) were calculated as described [7], using tryptophan as the standard ($\Phi = 0.14$). Excitation polarization spectra were obtained on an ISS K2 photon-counting spectrofluorimeter with the emission at $\lambda > 330$ nm viewed through a Schott WG345 (Schott Glass Technology, INC, Duryea, Pensylvania) cut-on filter. All measurements were done at 20 °C.

A LED (ISS, Champaign, IL.) centered at 294 nm was used for excitation for the lifetime measurements. The emission was collected through a Schott WG320 long-pass filter (Schott Glass Technology, INC, Duryea, Pensylvania). Phase and modulation values were measured and analyzed as described [24–26].

Globals Unlimited software (Urbana, IL) was used for the analysis with a constant, frequency-independent, standard deviation of 0.2° for phase and 0.004 for modulation. Goodness-of-fit was judged from the value of the reduced χ^2. The lifetime reference compound was *p*-terphenyl in ethanol ($\tau = 1.05$ ns) [27].

In the acrylamide quenching studies, the intensity of fluorescence at 20 °C was measured, excitation was at 295 nm, and samples were dissolved in Buffer B. The wavelength of the emission maximum did not change significantly with quencher concentration. The fluorescence intensities were corrected for inner filter effects, and the following modified Stern — Volmer equation [28] was fit to the F_0/F ratio

$$\frac{F_0}{F} = (1 + K_{SV}Q)e^{VQ} = (1 + k_q\tau_0 Q)e^{VQ}, \tag{3}$$

where F_0 and F are the fluorescence intensities in the absence and presence of quencher, respectively, k_q is the collisional bimolecular rate constant, τ_0 is the fluorophore lifetime in the absence of quencher, Q is the molar concentration of quencher, V is a parameter related to the probability of finding a molecule of quencher within the sphere of static quenching, and K_{SV} is the Stern Volmer constant.

Simulation of F_0/F as a function of Q for a multi-tryptophan protein was performed using the equation given by Eftink [28],

$$\frac{F_0}{F} = \frac{1}{\sum_i \frac{fi}{1 + K_i Q e^{V_i Q}}}, \tag{4}$$

and calculating f_i, the fraction of the emission due to the component *i*, as $F_{0i}/\sum F_{0i}$, where $F_{0i} = k_{ins}\,\varepsilon_i\,\Phi_i$ [29], k_{ins} is an instrumental constant that includes all the experimental settings of the measurement (but this term cancels out in the quotient), and ε_i is the extinction coefficient at the excitation wavelength of component *i*.

The efficiency of energy transfer (E) between the tryptophan residues was calculated from three-dimensional coordinates extracted from the Protein Data Bank (4BLM.pdb) [1], and using the following equations:

$$E = \frac{R_0^6}{R_0^6 + R^6}, \tag{5}$$

where R is the distance between the donor and the acceptor, and R_0 is the distance at which energy transfer is 50% calculated as

$$R_0^6 + 8.79 \times 10^{-25} n^{-4} \Phi_D \kappa^2 J_{AD} \tag{6}$$

In Eq. (6) n is the refractive index of the medium taken as 1.5, Φ_D is the quantum yield of the donor in the absence of the acceptor, κ^2 is the ^1L_a-^1L_a dipole–dipole orientation factor, and J_{AD} is the spectral overlap integral between the emission spectrum of the donor and the absorption spectrum of the acceptor,

$$\kappa^2 = (\cos\theta_T - 3\cos\theta_D \cos\theta_A)^2, \tag{7}$$

and

$$J_{AB} = \frac{\int F_D(\lambda)\epsilon_A(\lambda)\lambda^4 d\lambda}{\int F_D(\lambda)\, d\lambda} \tag{8}$$

In Eq. (7) and (8), θ_D and θ_A, are the angles between the emission dipole of the donor and the absorption dipole of the acceptor, θ_T is the angle between θ_D and θ_A and the vector joining the midpoints of the CE2-CD2 bond of the donor and the acceptor, respectively, and $F_D(\lambda)$ and $\varepsilon_A(\lambda)$ are the emission and absorption spectra of the donor and acceptor, respectively.

Wavelengths were expressed in nm, and therefore J_{AB} has units of $M^{-1}\,cm^{-1}\,nm^4$ and R is in Å. The direction of the transition moment of the ^1L_a state was considered to be −38° from a vector joining the midpoint of the CE2-CD2 bond and CD1 [30]. The ^1L_b dipole was not taken into account in the calculation of κ^2 since absorption and fluorescence at 295 nm are mainly from ^1L_a transitions [31].

3. Results

3.1. Protein purification and general characterization

ESP and the tryptophan variants showed excellent expression behavior, allowing the recovery of 100–250 mg of soluble protein per liter of culture. Judging from SDS-PAGE analysis, the proteins were purified to >98% homogeneity. The tryptophan replacements were corroborated by sequencing the expression plasmid and by mass analysis of the purified product (not shown).

The hydrodynamic properties of the purified enzymes were as expected for nearly spherical monomers the size of ESP (Table 1). The enzymic activity assays indicated that ESP^{W210}, ESP^{W229}, ESP^{W251}, ESP$^{\Delta W}$ posses 83, 84, 57, and 62%, respectively of the wild type specific activity (Table 1). The low impact of the mutations on the enzymic activity ensures that the overall native conformation is preserved in the variants [6,11]. The comparison of the k_{cat}, K_M, and k_{cat}/K_M values further reveals that Trp 229 and Trp 251, which are lacking in ESP^{W210}, can be replaced by phenylalanine with negligible active site perturbation. The changes of Trp 210 and Trp 229 in ESP^{W251} and Trp 210 and Trp 251 in ESP^{W229} have mild effects on catalysis. Considering that ESP^{W229} and ESP^{W251} have in common the replacement of Trp 210 and that replacement of Trp 251 (as in ESP^{W210}) has almost no effect on the catalytic parameters, it can be concluded that only the replacement of Trp 210 perturbs slightly the active site. This perturbation may be accounted for by the vicinity of the mutated residue to the catalytic center. Interestingly, the effect of replacing Trp 210 can be lessened by replacing also Trp 251 and Trp 229, as the triple mutant has catalytic parameters more like those of wild type ESP

Table 1
Hydrodynamic and catalytic properties.

Variant	R_S	k_{cat}	K_M	(k_{cat}/K_M)	Specific activity[a]
	(Å)	($10^3\ s^{-1}$)	(10^{-3} M)	($10^7\ s^{-1}\ M^{-1}$)	(%)
ESP	25.3 ± 0.7	3.06 ± 0.13	0.18 ± 0.05	1.7	100
ESP^{W210}	24.5 ± 1.2	2.06 ± 0.09	0.13 ± 0.05	1.6	83
ESP^{W229}	24.6 ± 1.3	2.09 ± 0.17	0.58 ± 0.02	0.4	84
ESP^{W251}	24.7 ± 0.6	1.40 ± 0.10	0.47 ± 0.03	0.3	57
ESP$^{\Delta W}$	25.0 ± 1.0	1.54 ± 0.06	0.26 ± 0.01	0.6	62

Values are the average of 2–3 measurements ± SEM.
[a] Percentage of the wild type ESP k_{cat}.

than ESP^{W229} or ESP^{W251}. This observation might reflect a compensating, subtle, and diffuse change in the conformational dynamics of $ESP^{\Delta W}$.

The effect of tryptophan replacement on the stability of ESP was assessed by equilibrium thermal unfolding monitored by the ellipticity at 220 nm (see Fig. A1 and Table A1 in Appendix A, Supplementary Information). ESP and the mutants behaved reversibly, with more than 95% percent recovery of the original signal upon cooling (not shown). A similar percentage of recovery was observed by measuring the enzymatic activity of samples subjected to the unfolding protocol (not shown). Thus, an equilibrium condition was assumed for the analysis, and the corresponding thermodynamic parameters were derived. For ESP, ESP^{W210}, and ESP^{W251} the ΔCp values were close to 4 kcal mol^{-1} K^{-1}, which is compatible with the expected increase of exposed area upon unfolding [32] and with the value obtained for ESP in differential scanning calorimetry experiments (V. A. Risso and M. R. Ermácora, unpublished results). The ΔCp value for ESP^{W229} is somewhat lower, which may indicate a difference in the states populated by this variant during unfolding.

The thermal stability of ESP is close to 7 kcal mol^{-1}, and the mutants are destabilized by 1–2 kcal mol^{-1} compared to ESP. We reported before that the stability of the wild-type protein decreases distinctly as a function of pH between 6.0 and 8.0 [8]. We found that the same happens with the tryptophan mutants. Thus, this behavior is a distinct feature of the three dimensional structure of ESP.

3.2. UV-absorption studies

To enhance the fine structure and facilitate the assignment of overlapping bands, the UV absorption spectra of ESP and model compounds were subjected to fourth-derivative analysis (Fig. A2 in Appendix A, Supplementary Information) [33]. The 250 and 270 nm region of the spectra is dominated by the vibronic structure of phenylalanine (Table A2, in Appendix A, Supplementary Information) and showed that for ESP and its variants, the phenylalanine bands are equally positioned and red-shifted by ~1 nm compared to the model of fully solvated phenylalanine. Thus, the native non polar environment of these residues is preserved in the mutants.

Between, 270 and 295 nm, multiple tyrosyl and tryptophanyl bands overlap and cannot be fully resolved. Yet, the contribution of tyrosine is limited to the maxima between 270 and 285 nm (Table A3, in Appendix A, Supplementary Information), and a tentative assignment of some of the bands in that spectral region and qualitative comparisons between variants could be performed. The data suggest that the tyrosine residues in ESP and the variants are in at least two distinct environments, both considerably more hydrophobic than that experienced by *N*-acetyl-L-tyrosinamide (NATyrA) in water.

The 290–310 nm region is dominated by ^1L_a and ^1L_b bands of tryptophan absorption, and the ^1L_a band is highly informative on the solvent environment of the chromophore. However, due to the low molar extinction coefficient and broadness of ^1L_a bands, fourth derivative spectra are not well-suited for the analysis. Therefore, the tryptophan UV contributions were calculated as the spectral difference between the ESP variants and $ESP^{\Delta W}$ (Fig. A3, in Appendix A, Supplementary Information), and a sum of Gaussians terms was fit to each difference spectra (Table A4, in Appendix A, Supplementary Information). The same fit was performed on the spectrum of *N*-acetyl-L-tryptophanamide (NATrpA), yielding results that are in excellent agreement with the vibronic structure reported previously for this compound and other indolyl derivatives [34]. The λ_{max} of the vibronic tryptophanyl bands in the ESP variants are red-shifted about 2 nm compared to the model compound in water, as expected for tryptophan residues with low solvent exposure in a folded protein. In this regard, ESP^{W210} and ESP^{W229} tryptophans appear to be in a unique environment, very similar for the two of them. On the contrary, the analysis shows clear evidence of at least two different environments for the tryptophan in ESP^{W251}. These environments result in ^1L_b and ^1L_a bands similar to those of the other two variants and in additional ^1L_b and ^1L_a bands even more red-shifted. The magnitude of the red shift for the additional bands suggests an alternative local conformation for Trp 251 in which the indolyl moiety establishes a distinct interaction with a polar or charged group [35,36]. Fitting the spectrum of wild-type ESP was not attempted. However, qualitative comparison of the red edges of the difference spectra clearly indicates that the alternative Trp 251 environment is not significantly populated in wild type ESP (not shown).

Far-UV CD spectra of the mutant proteins are similar in shape and intensity to that of the wild-type protein (Fig. 2). Since tryptophan residues contributes to the far-UV signal regardless the secondary structure [18], small changes of rotatory power for the mutants is to be expected because of the differences in tryptophan content. Therefore, the secondary structure in these variants is likely to be largely preserved. Overall inspection of the near-UV CD spectra indicates that most of the rotatory power of ESP is due to tryptophan absorption. The weaker CD signal comes from $ESP^{\Delta W}$, which may be explained by the low intrinsic rotatory power of phenylalanine residues and the low rotatory power contribution of ESP tyrosine residues. In this regard, the individual tyrosine bands in ESP seem to cancel out, a frequent outcome in proteins with multiple tyrosines [35].

The fine structure of the CD spectra is in general agreement with the vibronic components in the absorption spectra (see above). However, CD additionally shows that Trp 210 and Trp 229 contribute

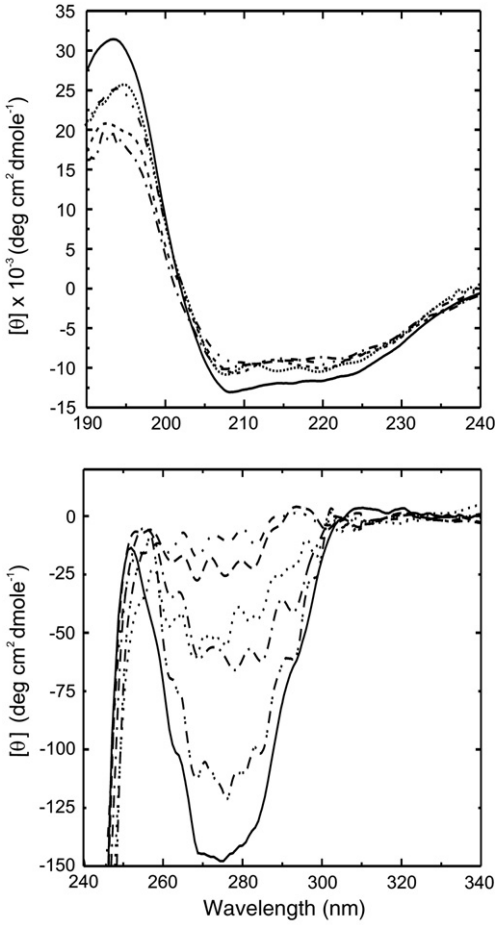

Fig. 2. CD spectra. ESP (full line), ESP^{W210} (– · –), ESP^{W229} (· · ·), ESP^{W251} (– – –), and $ESP^{\Delta W}$ (· – – ·) spectra are plotted in the upper (far UV) and lower (near UV) panels. A wild-type ESP near-CD spectrum calculated from the contributions of the individual mutants ($ESP^{W210} + ESP^{W229} + ESP^{W251} - 2 \times ESP^{\Delta W}$) is also shown (– · · · –) in the lower panel. Ellipticity values are per decimole of amino acid residue.

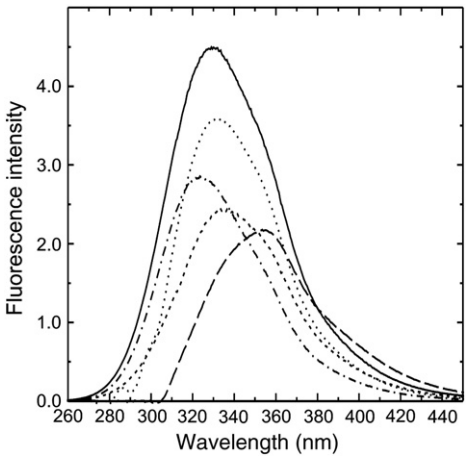

Fig. 3. Steady-state fluorescence spectra. The spectra of ESP (solid line), ESP^{W210} (– · –), ESP^{W229} (· · ·), ESP^{W251} (– – –), and NATrpA (— — —) are shown. The signals were normalized by the corresponding UV absorption at 295 nm.

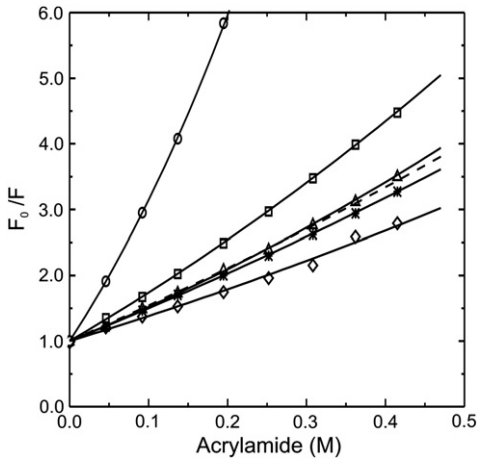

Fig. 4. Acrylamide quenching of fluorescence. Data for l-tryptophan (circles), ESP^{W210}, (rhombuses), ESP^{W229} (squares), ESP^{W251} (crosses), and ESP (triangles) are plotted. Eq. (3) was fit to the data, and the relevant parameters are listed in Table 2. The theoretical curve for the ESP (dashes) was calculated with Eq. (4) [28].

strong and negative ^1L_b band at 291–293 nm, whereas Trp 251 exhibits very low rotatory power. Finally, the algebraic sum of the tryptophan components in the spectra of each variant and the CD spectra of ESP$^{\Delta W}$ account for most of the intensity and fine structure of the wild type ESP spectrum.

3.3. Fluorescence

The different chemical environments of the ESP tryptophan residues are indicated by the fluorescence λ_{max} and Φ values (Fig. 3, Table 2). Compared with NATrpA in water ($\lambda_{max}=356$ nm), ESP^{W210} shows a 33 nm blue shift. The shift is less, about 23 nm, for ESP^{W229} and ESP^{W251}. These blue shifts are consistent with the degree of solvent exposure of each tryptophan residue in the X-ray structure.

The Φ value of ESP is typical of proteins with buried tryptophans experiencing a moderate degree of quenching. In a multi-tryptophan protein, the Φ value of a particular tryptophan can be estimated from the Φ value of the corresponding single tryptophan mutant. This estimation, however, assumes ideal behavior, the absence of conformational changes derived from the residue substitution, and the lack of fluorescence loses due to interactions be tween the removed and preserved tryptophans. On the other hand, the theoretical Φ value of a multi-tryptophan protein can be calculated as an extinction-coefficient-weighted average of the Φ values of the individual tryptophans [37]. The ESP mutants have Φ values ranging 0.16–0.21, none is larger than that of the wild type protein. The calculated Φ average is 0.18, which accounts for 70% of the wild-type Φ. These results suggest that there are no strongly quenched ('dark') tryptophan residues in ESP.

Frequency-domain measurements yielded the lifetimes of the tryptophan residues in each mutant and the wild-type protein (Table 2). Decays were satisfactorily fit to a sum of discrete exponentials. A component with a lifetime of 5—6 ns characterizes 87-96% of the signal for wild-type ESP and all the single tryptophan variants. The residual fraction, in all cases, is from a component of 0.7—1.3 ns.

The rate of radiative and nonradiative decay can be calculated from lifetime and quantum yield data (Table 2). ESP variants have similar radiative decay rates, somewhat smaller than that of wild type ESP. Conversely, the nonradiative rates of the ESP variants are slightly larger than that of wild type ESP. These differences, although small, suggests that the mutations alters the conformational dynamics of ESP.

The accessibility of ESP tryptophan residues to acrylamide was also characterized (Fig. 4). Since the plot $F_0/F=f(Q)$ exhibits no negative curvature it is concluded that the fraction of tryptophan residues which are inaccessible to acrylamide is negligible. The slightly positive curvature of the plot indicates a moderate static quenching. In this cases, a modified form of the Stern-Volmer relationship adequately describe the total quenching process (Eq. (3)) [28]. In this model the kinetics of the quenching reaction is operationally dissected into

Table 2
Fluorescence properties.

Variant	Φ[a]	λ_{max} (nm)	τ[b] (ns)	f[c]	χ^2[d]	k_{nr}[e] (10^8 s^{-1})	Γ[e] (10^8 s^{-1})	K_{SV}[f] (M^{-1})	k_q[f] (10^9 M^{-1} s^{-1})	V[f] (M^{-1})	ASA[g] (%)
ESP	0.26 ± 0.02	334.0	5.98	0.96	0.52	1.24	0.43	4.44	0.74	0.52	2.3, 16.1, 11.9
			1.26	0.04							
ESP^{W210}	0.17 ± 0.03	323.5	5.15	0.90	1.10	1.61	0.33	3.36	0.67	0.33	2.3
			1.34	0.10							
ESP^{W229}	0.21 ± 0.02	332.0	5.96	0.87	1.99	1.33	0.35	6.68	1.12	0.42	16.1
			0.58	0.13							
ESP^{W251}	0.16 ± 0.03	333.5	5.68	0.88	1.34	1.48	0.28	4.57	0.80	0.29	11.9
			0.74	0.12							

[a] Determined by steady state fluorescence as described in Material and methods.
[b] Intensity decays were fit to a biexponential model $I(t)=\alpha_1\exp(-t/\tau_1)+\alpha_2\exp(-t/\tau_2)$.
[c] The fraction of fluorescence emission ascribed to a given tryptophan was calculated as $f_i=\alpha_i\,\tau_i/\sum_j \alpha_j\,\tau_j)$.
[d] χ^2 is the reduced chi-square value corresponding to the fit of the phase and modulation data.
[e] k_{nr} and Γ are the non-radiative and radiative rate decays, respectively.
[f] The quencher was acrylamide and the parameters are described in Eq. (1).
[g] Accessible surface area for the single tryptophan residue in each mutant calculated from the X-ray coordinates of ESP (4blm.pdb) with a 1.4-Å probe (see Material and methods).

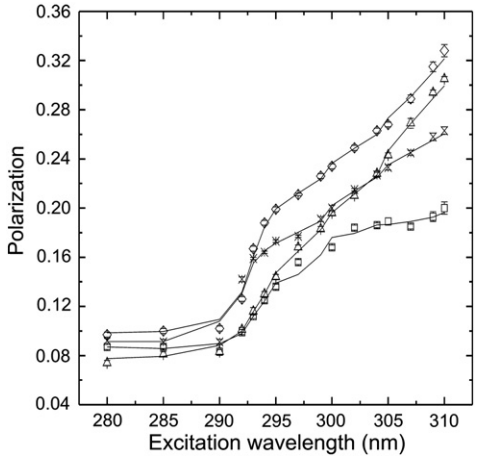

Fig. 5. Fluorescence polarization spectra of ESP (squares), ESP^{W210} (triangles), ESP^{W229}, (diamond), and ESP^{W251} (crosses). Each measurement was performed in triplicates and the bars represent the standard deviation.

collisional (K_{SV}) and static (V) components. The kinetic bimolecular constant for diffusion controlled encounter of the fluorophore and the quencher, k_q, can be calculated from the K_{SV} constant and the lifetime of fluorescence in the absence of quencher. V is related to the probability of a quencher molecule being at any time close enough to the excited fluorophore to result in extremely rapid quenching, i.e., quenching which occurs during a very small fraction of the excited state lifetime. Typical values for solvated tryptophanyl residues in unstructured peptides are $k_q = 4\times10^9\ M^{-1}\ s^{-1}$ and $V = 1\ M^{-1}$ [28], whereas for NATrpA the values determined for this work were $k_q = 5.7\times10^9\ M^{-1}\ s^{-1}$ and $V = 1.5\ M^{-1}$. For totally inaccessible tryptophanyl residues, however, these parameters can have values as small as $5\times10^7\ M^{-1}\ s^{-1}$ and ~0 M^{-1} [28]. In ESP and its variants, the values are $k_q = 0.7\text{–}1.1\times10^9\ M^{-1}\ s^{-1}$ and $V = 0.3\text{–}0.5\ M^{-1}$, which are consistent with low tryptophan solvent exposure as suggested from the X-ray coordinates of ESP (Table 2). In all cases, an increase in the quenching rate was observed with an increase in temperature, which is typical of quenching processes predominantly mediated by diffusion (not shown) [15]. Most importantly, a numerical simulation (Eq. (4)) [28], assuming additive behavior of independent tryptophan residues with the K_{SV} and k_Q values determined for the ESP variants, yielded a F_0/F curve in excellent agreement with the experimentally determined values for ESP (Fig. 4).

A relevant question regarding ESP fluorescence is whether the tryptophanyl residues can undergo Förster resonance energy transfer (FRET) one to another. Gaviola and Pringsheim first established that energy homotransfer can contribute to fluorescence depolarization and Weber later demonstrated that such homotransfer can occur between indole molecules and moreover that the homotransfer, and consequently depolarization, is greatly diminished by exciting at the red edge of the absorption spectrum [38–40]. The existence of FRET between tryptophanyl groups can therefore be established comparing the polarization ensuing excitation at different wavelengths [41]. The polarization of the emission as a function of the excitation wavelength for ESP and its variants are shown in Fig. 5. Measurement above 310 nm could not be performed with sufficient accuracy due to technical limitations and the curves fail to reach the high polarization plateau. Nonetheless, the curves for the ESP variants show clearly a much larger polarization than wild type ESP in the 295–310 nm region. The most likely explanation for this is the existence of significant energy transfer between Trp residues in the latter.

The theoretical efficiency of energy homotransfer between tryptophans can be calculated from geometric parameters and the absorption and fluorescence spectra. The results of such calculation for ESP and its variants are given in Table 3. Tryptophans 229 and 251 are the closest in space (10 Å) and for them energy transfer is calculated to be 55–69%. The following pair in distance is that of Trp 210–Trp 251, and in this case energy transfer is estimated to be no larger than 13%. Finally, residues Trp 210 and Trp 229 are almost 24 Å apart and energy transfer between them should be less than 10%.

Table 3
Tryptophan to tryptophan energy transfer parameters.

D→A[a]	R[b] (Å)	κ^2[c]	J_{AD}[c] (10^{-16} cm^6 mmol^{-1})	R_0[c] (Å)	E[c]
210→229	23.8	0.800	4.59	15.82	0.08
229→210	23.8	0.800	1.46	13.54	0.03
210→251	15.3	0.049	9.00	11.11	0.13
251→210	15.3	0.049	2.84	9.08	0.04
229→251	10.3	0.137	3.66	11.76	0.69
251→229	10.3	0.137	2.69	10.68	0.55

[a] Donor–acceptor pair.
[b] Distance between the centers of CD2–CE2 bonds of each Trp–Trp pair according to the X-ray structure.
[c] Parameters calculated using Eqs. (5)–(8) and defined in the text.

4. Discussion

Three single-tryptophan and one tryptophan-less ESP variants have been designed and prepared with the aim of identifying and characterizing specific spectroscopic features that may help monitoring the conformational transitions of this protein with subdomain resolution. To serve as intended, the conformational equivalence of these variants needed to be corroborated, and the results presented herein establish that this condition was fulfilled. The strongest evidence in this regard is perhaps the extent of the variant preservation of the native enzymic activity, a feature that is exquisitely dependent on even minor conformational alterations. However, equally reassuring is that the main near-UV CD, steady state fluorescence, and acrylamide quenching properties of the wild type protein can be accounted for by the properties of the tryptophan variants.

Moreover, for a meaningful comparison, the thermodynamic properties of the ESP mutants needed to be in harmony with those of wild-type ESP. Herein is also demonstrated that the thermal stability of ESP is lowered less than 2 kcal mol^{-1} as the results of the mutations. Since ESP is an exceedingly stable protein, the changes have no significant impact on the native state population.

The near UV CD spectrum of ESP is dominated by the transitions of Trp 210 and 229. Both give rise to strong negative signals. The contribution of Trp 251 is very weak and of opposite sign. The contribution of tyrosine and phenylalanine residues to the CD is also very weak, which is likely due to signal cancellation of negative and positive peaks. This is an important piece of information because it must be concluded that monitoring the conformational transitions of ESP by near UV CD yields information mostly limited to the tertiary structure around Trp 210 and 229, in the core of the two lactamase domain (Fig. 1). Conformational changes at the interface between the two domains, where Trp 251 is located, are likely silent in near-UV CD measurements.

To find ways to monitor other regions of the protein, we paid close attention to the UV absorption properties. Many of the vibronic details for the spectra of these residues were drawn by numerical processing and are provided (see Tables A2–A4, in Appendix A, Supplementary Information). To illustrate the usefulness of such data, it is worth to mention that, as described in Results, they revealed a subtly different conformational context for Trp 251 in ESP^{W251}.

FRET between tryptophan residues is a well documented phenomenon [42]. We found that the energy absorbed by Trp 210 is dissipated by fluorescence emission or nonradiative decay with little homotransfer to the other tryptophans. On the contrary, Trp 229 and Trp 251 must be considered as an interdependent fluorescence couple that cannot be excited independently when they are present in the

same native molecule. These details must be taken into consideration when following ESP conformational changes using its fluorescence as a probe.

Most of the α domain of ESP is a bundle of six α helices, five placed as the staves of a barrel and surrounding the sixth (see Fig. 1). Trp 210 is located at the hydrophobic interface between the central and two of the peripheral helices. Thus Trp 210 is ideally suited for monitoring the conformational dynamic of the α domain, and its contribution to fluorescence can be considered independent of the conformation of α + β domain.

Trp 210 is highly conserved among class A β-lactamases and its fluorescence properties have been used to characterize early folding intermediates in the folding pathway of TEM-1 β-lactamase [43]. This characterization was possible because in TEM-1 β-lactamase, the fluorescence of Trp 210 in the native state is strongly quenched by a nearby disulfide bond, making directly observable the formation of the α-domain by a time-dependent decrease in fluorescence emission. The disulfide is not present in ESP, and the present work shows that Trp 210 contributes about one third of the emission in the native state, that it has the bluest emission maximum of the three tryptophan residues, and that it does not engage in significant energy transfer to the other two tryptophan residues.

Other interesting features of Trp 210 are a low solvent accessibility calculated from the X-ray coordinates, a rate of non-radiative decay of fluorescence somewhat larger than those of Trp 229 and Trp 251, and a small bimolecular quenching constant for acrylamide. A likely explanation for these features can be drawn examining the seven available X-ray structures of *B. licheniformis* class A β-lactamases (not shown). The superposition of these structures reveals that Trp 210 is in a very rigid, solvent-shielded context, with very low *rmsd* between the different structures. In addition, the *B-factors* of the atoms in the vicinity of Trp 210 are quite low. Thus, the low local conformational dynamics and the steric hindrance explain the poor diffusion of the quencher to the interior of the α-domain. On the other hand, the enhanced rate of non-radiative decay may arise from several specific interactions: a water molecule hydrogen-bonded to Asp 209 is kept at van der Waals distance from the center of the benzene ring, and NE1 is at hydrogen bond distance from two water molecules and from OD2 of Asp 124.

Trp 229 is also highly conserved among class A lactamases, and because of its location it reports on the conformational integrity of the α + β domain and particularly on the parallel placement of the two α-helical termini of the protein. Trp 229 has the highest Φ among ESP tryptophan residues, a blue shifted emission, the largest acrylamide quenching, and along with Trp 210 accounts for most of the fluorescence intensity and near UV CD signals. These properties can be rationalized taken into account that Trp 229 is in a more dynamic environment than Trp 210: (a) in all seven structures the *B-factors* are distinctly higher for the β-turn comprising residues 226-229 and so are the *rmsd* values for the superimposition; (b) no polar side chains and only one water molecule are within van der Waals distance of the aromatic ring of Trp 229, the later making an hydrogen bond to NE1. The conformational fluctuations may thus explain the higher diffusion of acrylamide and the low polarity of the environment may explain both the blue-shift and the high Φ. Unfortunately, in the wild type molecule, the fluorescence of Trp 229 is not insulated from the fluorescence of Trp 251: these two tryptophans participate in significant homotransfer reactions and excitation of one is accompanied by emission from the other. Thus, the only suitable variant to monitor specific conformational changes of the α + β domain is ESP^{W229}.

Trp 251 reports on the hydrophobic interface formed as the two domains come into contact in the native state. There is no equivalent to Trp 251 in TEM-1 β-lactamases. On one hand, this tryptophan residue has a low Φ – close to the value of fully solvated tryptophan – a comparatively red-shifted emission maximum, and a rate of bimolecular acrylamide quenching mid-way between those of Trp 210 and Trp 229. These properties may be explained as follows: (a) although the calculated static solvent accessibility of Trp 251 is low, judging from the *B-factors* and *rmsd* values, Trp 251 is located at the beginning of a fluctuating loop (residues 252-257); and (b) the environment of Trp 251 is dominated by one water molecule and two charged side chains at van der Waals distance (Lys 212 and Glu 230; at 4-5 and 6 Å, respectively from the aromatic ring).

5. Conclusion

This work describes the design and thorough spectroscopic characterization of tryptophan variants of ESP suited for assessing the conformational details and dynamics of specific substructures of the protein. Several of the spectroscopic features have been related to specific details of the three-dimensional structure and dynamic. Therefore, the results presented herein will allow the interpretation of the conformational transitions and fluctuations of ESP and other class A β-lactamases with subdomain resolution.

Acknowledgments

This work was supported by grants from CONICET, UNQ, and ANPCyT.

Appendix A. Supplementary data

Supplementary data associated with this article can be found, in the online version, at doi:10.1016/j.bpc.2010.05.013.

References

[1] P.C. Moews, J.R. Knox, O. Dideberg, P. Charlier, J.M. Frère, Beta-lactamase of *Bacillus licheniformis* 749/C at 2 Å resolution, Proteins 7 (1990) 156–171.
[2] W.A. Escobar, A.K. Tan, E.R. Lewis, A.L. Fink, Site-directed mutagenesis of glutamate-166 in beta-lactamase leads to a branched path mechanism, Biochemistry 33 (1994) 7619–7626.
[3] E.R. Lewis, K.M. Winterberg, A.L. Fink, A point mutation leads to altered product specificity in beta-lactamase catalysis, Proc. Natl Acad. Sci. USA 94 (1997) 443–447.
[4] E.J. Lietz, H. Truher, D. Kahn, M.J. Hokenson, A.L. Fink, Lysine-73 is involved in the acylation and deacylation of beta-lactamase, Biochemistry 39 (2000) 4971–4981.
[5] M.C. Frate, E.J. Lietz, J. Santos, J.P. Rossi, A.L. Fink, M.R. Ermácora, Export and folding of signal-sequenceless *Bacillus licheniformis* beta-lactamase in *Escherichia coli*, Eur. J. Biochem. 267 (2000) 3836–3847.
[6] V.A. Risso, M.E. Primo, M.R. Ermácora, Re-engineering a beta-lactamase using prototype peptides from a library of local structural motifs, Protein Sci. 18 (2009) 440–449.
[7] J. Santos, L.G. Gebhard, V.A. Risso, R.G. Ferreyra, J.P. Rossi, M.R. Ermácora, Folding of an abridged beta-lactamase, Biochemistry 43 (2004) 1715–1723.
[8] J. Santos, V.A. Risso, M.P. Sica, M.R. Ermácora, Effects of serine-to-cysteine mutations on beta-lactamase folding, Biophys. J. 93 (2007) 1707–1718.
[9] P. Ledent, C. Duez, M. Vanhove, A. Lejeune, E. Fonze, P. Charlier, F. Rhazi-Filali, I. Thamm, G. Guillaume, B. Samyn, B. Devreese, J. Van Beeumen, J. Lamotte-Brasseur, J.M. Frere, Unexpected influence of a C-terminal-fused His-tag on the processing of an enzyme and on the kinetic and folding parameters, FEBS Lett. 413 (1997) 194–196.
[10] D.B. Ureta, P.O. Craig, G.E. Gomez, J.M. Delfino, Assessing native and non-native conformational states of a protein by methylene carbene labeling: the case of *Bacillus licheniformis* beta-lactamase, Biochemistry 46 (2007) 14567–14577.
[11] L.G. Gebhard, V.A. Risso, J. Santos, R.G. Ferreyra, M.E. Noguera, M.R. Ermacora, Mapping the distribution of conformational information throughout a protein sequence, J. Mol. Biol. 358 (2006) 280–288.
[12] M.R. Eftink, Use of fluorescence spectroscopy as thermodynamics tool, Meth. Enzymol. 323 (2000) 459–473.
[13] M.R. Eftink, R. Ionescu, G.D. Ramsay, C.Y. Wong, J.Q. Wu, A.H. Maki, Thermodynamics of the unfolding and spectroscopic properties of the V66W mutant of *Staphylococcal nuclease* and its 1–136 fragment, Biochemistry 35 (1996) 8084–8094.
[14] S. Chakraborty, V. Ittah, P. Bai, L. Luo, E. Haas, Z. Peng, Structure and dynamics of the alpha-lactalbumin molten globule: fluorescence studies using proteins containing a single tryptophan residue, Biochemistry 40 (2001) 7228–7238.
[15] J.R. Lakowicz, Principles of Fluorescence Spectroscopy, Kluwer Academic/Plenum Publishers, New York, 1999.
[16] S.M. Kelly, N.C. Price, The use of circular dichroism in the investigation of protein structure and function, Curr. Protein Pept. Sci. 1 (2000) 349–384.
[17] E.M. Clerico, M.R. Ermácora, Tryptophan mutants of intestinal fatty acid-binding protein: ultraviolet absorption and circular dichroism studies, Arch. Biochem. Biophys. 395 (2001) 215–224.
[18] R.W. Woody, A.K. Dunker, in: G.D. Fasman (Ed.), Circular Dichroism and the Conformational Analysis of Biomolecules, Plenum Press New York and London, New York and London, 1996, pp. 109–157.

[19] J.A.T. Jansson, A direct spectrophotometric assay for penicillin ß-lactamase (penicillinase), Biochim. Biophys. Acta 99 (1965) 171–172.
[20] F.M. Richards, Areas, volumes, packing and protein structure, Annu. Rev. Biophys. Bioeng. 6 (1977) 151–176.
[21] V.N. Uversky, G.V. Semisotnov, R.H. Pain, O.B. Ptitsyn, 'All-or-none' mechanism of the molten globule unfolding, FEBS Lett. 314 (1992) 89–92.
[22] A.R. Fersht, Structure and Mechanism in Protein Science: A Guide to Enzyme Catalysis and Protein Folding, Freeman, New York, 1999.
[23] W.H. Press, S.A. Teukolsky, W.T. Vetterling, B.P. Flannery, C The Art of Scientific computing, Cambridge University Press, New York, 1992.
[24] R.D. Spencer, G. Weber, Measurements of sub-nanosecond fluorescence lifetime with a cross-correlation phase fluorometer, Ann. NY Acad. Sci. 158 (1969) 361–376.
[25] D.M. Jameson, E. Gratton, R.D. Hall, The measurement and analysis of heterogeneous emission by multifrequency phase and modulation spectroscopy, Applied Spectroscopy Review 20 (1984) 55–105.
[26] D.M. Jameson, T.L. Hazlet, Biophysical and Biochemical Aspects of Fluorescence Spectroscopy, Plenum Press, New York, 1991.
[27] D.M. Jameson, E. Gratton, G. Weber, B. Alpert, Oxygen distribution and migration within Mbdes Fe and Hbdes Fe. Multifrequency phase and modulation fluorometry study, Biophysical Journal 45 (1984) 795–803.
[28] M.R. Eftink, C.A. Ghiron, Exposure of tryptophanyl residues in proteins. Quantitative determination by fluorescence quenching studies, Biochemistry 15 (1976) 672–680.
[29] C.R. Cantor, P.R. Schimmel, Biophysical Chemistry. Part II: Techniques for the Study of Biological Structure and Function, W. H. Freeman and Company, New York, 1980.
[30] Y. Yamamoto, J. Tanaka, Polarized absorption spectra of crystals of indole and its related compounds, Bull. Chem. Soc. Jpn 45 (1972) 1362–1366.
[31] P.R. Callis, ^{1}La and ^{1}Lb transitions of tryptophan: applications of theory and experimental observations to fluorescence of proteins, Meth. Enzymol. 278 (1997) 113–150.
[32] J.K. Myers, C.N. Pace, J.M. Scholtz, Denaturant m values and heat capacity changes: relation to changes in accessible surface areas of protein unfolding, Protein Sci. 4 (1995) 2138–2148.
[33] E. Padros, A. Morros, J. Manosa, M. Dunach, The state of tyrosine and phenylalanine residues in proteins analyzed by fourth-derivative spectrophotometry. Histone H1 and ribonuclease A, European Journal of Biochemestry 127 (1982) 117–122.
[34] E.H. Strickland, J. Horwitz, E. Kay, L.M. Shannon, M. Wilchek, C. Billups, Near-ultraviolet absorption bands of tryptophan. Studies using horseradish peroxidase isoenzymes, bovine and horse heart cytochrome c, and N-stearyl-L-tryptophan n-hexyl ester, Biochemistry 10 (1971) 2631–2638.
[35] E.H. Strickland, Aromatic contributions to circular dichroism spectra of proteins, CRC Crit. Rev. Biochem. 2 (1974) 113–175.
[36] T.A. Bewley, C.H. Li, Conformational comparison of human pituitary growth hormone and human chorionic somatomammotropin (human placental lactogen) by second-order absorption spectroscopy, Arch. Biochem. Biophys. 233 (1984) 219–227.
[37] A. Sillen, Y. Engelborghs, The correct use of 'average' fluorescence parameters, Photochem. Photobiol. 67 (1998) 475–486.
[38] E. Gaviola, P. Pringsheim, Infuses der Konzentration auf die Polarisation der Fluoreszenz von Farbstofflosenungen, Z Physik 24 (1924) 24–36.
[39] G. Weber, Fluorescence polarization spectrum and electronic-energy transfer in tyrosine. transfer in tyrosine, tryptophan and related compounds, Biochem. J. 75 (1960) 335–345.
[40] G. Weber, M. Shinitzky, Failure of energy transfer between identical aromatic molecules on excitation at the long wave edge of the absorption spectrum, Proc. Natl Acad. Sci. USA 65 (1970) 823–830.
[41] P.D. Moens, M.K. Helms, D.M. Jameson, Detection of tryptophan to tryptophan energy transfer in proteins, Protein J. 23 (2004) 79–83.
[42] R. Vos, Y. Engelborghs, J. Izard, D. Baty, Fluorescence study of the three tryptophan residues of the pore-forming domain of colicin A using multifrequency phase fluorometry, Biochemistry 34 (1995) 1734–1743.
[43] P. Gervasoni, A. Pluckthun, Folding intermediates of beta-lactamase recognized by GroEL, FEBS Lett. 401 (1997) 138–142.